ACS APPLIED MATERIALS & INTERFACES

Research Article

www.acsami.org

Bioactive Core–Shell Nanofiber Hybrid Scaffold for Efficient Suicide Gene Transfection and Subsequent Time Resolved Delivery of Prodrug for Anticancer Therapy

Uday Kumar Sukumar[†] and Gopinath Packirisamy[*,†,‡]

[†]Nanobiotechnology Laboratory, Centre for Nanotechnology, [‡]Department of Biotechnology, Indian Institute of Technology Roorkee, Roorkee, Uttarakhand-247667, India

Supporting Information

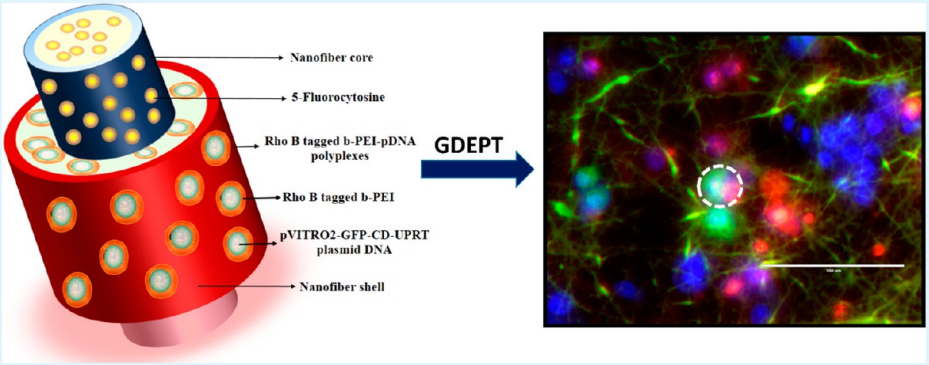

ABSTRACT: Nanofiber scaffold's ability to foster seemingly nonexistent interface with the cells enables them to effectively deliver various bioactive molecules to cells in the vicinity. Among such bioactive molecules, therapeutically active nucleic acid has been the most common candidate. In spite of such magnanimous efforts in this field, it remains a paradox that suicide gene delivery by nanofibers has never been sought for anticancer application. To investigate such a possibility, in the present work, a composite core–shell nanofiberous scaffold has been realized which could efficiently transfect suicide gene into cancer cells and simultaneously deliver prodrug, 5-Fluorocytosine (5-FC) in a controlled and sustained manner. The scaffold's ability to instigate apoptosis by suicide gene therapy in nonsmall lung cancer cells (A549) was ascertained at both phenotypic and genotypic levels. A cascade of events starting from suicide gene polyplex release from nanofibers, transfection, and expression of cytosine deaminase-uracil phosphoribosyltransferase (CD::UPRT) suicide gene by A549; subsequent prodrug release; and its metabolic conversion into toxic intermediates which finally culminates in host cells apoptosis has been monitored in a time-dependent manner. This work opens up new application avenues for nanofiber-based scaffolds which can effectively manage cancer prognosis.

KEYWORDS: *core–shell nanofibers, gene transfection, suicide gene, prodrug, anticancer therapy*

1. INTRODUCTION

The ease of polymer nanofiber fabrication and versatility of electrospinning by itself has catered wide scope for developing nanofiber based multifaceted drug delivery systems. At present, these electrospun nanofibers have already witnessed unparalleled share of success in controlled and sustained delivery of diverse bioactive molecules (i.e., drugs, siRNA, DNA, proteins, and nanoparticles). In recent years, apart from drugs, nucleic acid delivery by nanofibers has also been pursued extensively for gene therapy applications.[1] Such nanofiber based gene therapy approach by virtue of being localized administration owns a clear edge over other polymer based gene delivery formulations in terms of therapeutic index. Moreover, the controlled release of therapeutic nucleic acids from nanofibers renders scope for higher and prolonged dosages which otherwise remains elusive, and thereby it also does not tend to elicit systemic toxicity after administration. Apart from this, the extracellular matrix (ECM) look-alike morphology of nanofibers narrows the interface between the target cells and the therapeutic genes to be delivered.[2]

Although nanofiber based gene therapy has evolved its course for a decade, its use for suicide gene therapy (gene directed enzyme prodrug therapy (GDEPT)) has remained unexplored until now. The term "suicide gene therapy" by itself is readily comprehensible, which denotes delivery of gene encoding a functional enzyme which is not toxic per se but which potentiates the target cells to catalyze the conversion of therapeutically less active prodrug into highly toxic com-

Received: June 14, 2015
Accepted: August 3, 2015
Published: August 3, 2015

DOI: 10.1021/acsami.5b05280
ACS Appl. Mater. Interfaces 2015, 7, 18717–18731

pounds.[3] The toxic metabolic intermediates thereby generated certainly effectuate their therapeutic potential on the native cell and also tend to permeate into cells in the vicinity so as to mediate their bystander effects. Owing to such bystander effects, higher transfection efficiency does not remain a prerequisite anymore for complete eradication of tumors by suicide gene therapy. The use of suicide genes further confines the prodrug therapeutic potentials to the cells solely expressing appropriate enzyme (encoded by the suicide gene) which otherwise remain nontoxic unless otherwise acted upon by the enzymes.

A panoptic study of suicide gene strategies thus far has revealed various combinatorial enzyme-prodrug systems, of which thymidine kinase, cytosine deaminase, purine nucleoside phosphorylase (PNP) carboxypeptidase A1, and nitroreductase deserve mention owing to their significant success.[4] The present work thrusts on therapeutic potential of genetically engineered dual-enzyme suicide gene, CD::UPRT, and prodrug 5-FC. The enzyme cytosine deaminase (CD) converts 5-FC to 5-Fluorouracil (5-FU), a catabolic inhibitor of thymidine synthetase enzyme which stalls nucleic acid synthesis and which also leads to miss-incorporation of bases (i.e., mutations) and thereby triggers a cascade of signaling pathways which finally culminates in cellular apoptosis. Owing to poor 5-FU stability and lack of bystander effects in CD/5-FC enzyme-prodrug system, it does not attain significant therapeutic outcomes. Therefore, to further supplement the therapeutic potential of CD/5-FC system, another enzyme uracil phosphoribosyl transferase (UPRT) in also inculcated, which converts 5-FU into cytotoxic 5-fluorouracilmonophosphate (5-FUMP) which is later catalyzed to even more toxic byproducts 5-fluorodeoxyuracilmonophosphate (5-FdUMP) and 5-fluorouraciltriphosphate (5-FUTP).[5] Preexisting literature on targeted delivery of CD::UPRT suicide gene by means of mesenchymal stem cells further strengthens the therapeutic efficacy of the suicide gene (i.e., CD::UPRT) under study.[6,7] Taking into consideration such improved therapeutic prospects of CD::UPRT/5-FC system, its anticancer potentials are put to test in this work.

Among the various nonviral transfecting agents, polycationic polyethylenimine has drawn huge attention owing to its ability to efficiently condense DNA to form stable polyplexes.[8] Apart from this, branched polyethylenimine (bPEI) presence renders the polyplexes an ability to circumvent endosomal degradation by proton sponge effect and thereby delivers intact suicide gene to the cell cytoplasm.[9] Thrusting upon such prenotions, bPEI and pVITRO2-GFP/CD::UPRT plasmid polyplexes were synthesized at different nitrogen/phosphate (N/P) ratios for asserting a trade-off between polyplexes stability and transfection efficiency, the most appropriate of which was then incorporated within the nanofibers by blend electrospinning.

Efficient suicide gene therapy begins with suicide gene transfection into the host cell which is subsequently followed by administration of prodrug. In coherence with a similar trend, the present work evaluates core−shell nanofiberous scaffold for delivery of suicide gene and prodrug. Presynthesized suicide gene-bPEI polyplexes are loaded in the nanofiber shell by virtue of which they are predominantly released during the initial phase of incubation, and they transfect the cells in the vicinity, followed by sustained release of prodrug (5-FC) loaded in the nanofiber core. As pVITRO2-GFP/CD::UPRT-bPEI polyplexes and 5-FC are localized in different layers of core−shell nanofibers (outer shell and inner core of nanofiber, respectively), they follow a distinct release profile which is most appropriate for fostering anticancer potentials of suicide gene therapy. Differential cross-linking of nanofibers also extends the possibility of altering the polyplexes and prodrug release profile. Thus, this work envisions core−shell nanofibers as a versatile means of simultaneously delivering suicide gene and the prodrug in a controlled and sustained manner.

2. MATERIALS AND METHODS

Materials. Poly(ethylene oxide) (PEO) (M_V: 900 000) and branched poly(ethylenimine) (bPEI) (M_w: 25 000) were purchased from Sigma-Aldrich. Prodrug, 5-FC and fluorescent stains, propidium iodide (PI), and Hoechst 33342 were also procured from Sigma-Aldrich and were stored at appropriate temperature until used. *N*-(3-(dimethylamino)propyl)-*N*′-ethylcarbodiimide (EDC), *N*-hydroxysuccinimide (NHS), and cellulose dialysis membrane-132 (molecular weight cutoff (MWCO), 12 kDa) were acquired from HiMedia. Heparin sodium salt (extracted from bovine intestinal mucosa) and Deoxyribonuclease I (DNase I) (extracted from bovine pancreas) were purchased from SRL Pvt. Ltd., India. Fluorescent cellular probes, lysotracker green DND-26, and Rhodamine B (RhoB) were procured from life technologies and were used as per manufacture's instruction. 3-(4,5-Dimethylthiazol-2-yl)-2,5-diphenyltetrazolium bromide (MTT) was bought from Amresco life science, USA. PCR primers used in this work were ordered from Imperial Life Science, India. Other chemicals used in this work were analytical grade and were used as received without further modification. A549 (Non-Small Cell Lung Cancer) cells were received from National Centre for Cell Science, Pune, India. They were maintained in Dulbecco's modified Eagle's medium (DMEM) with 10% fetal bovine serum (FBS) and 1% penicillin-streptomycin in 37 °C incubator with 5% CO_2 and 95% air.

Synthesis of bPEI-RhoB Conjugates. The fluorescent RhoB was conjugated to bPEI by EDC and NHS coupling reaction. The free −COOH groups of RhoB were covalently linked to primary amine ($-NH_2$) groups at the terminal of bPEI by amide bonds. As an initial activation step, free amine groups of bPEI (0.1 g) were deprotonated in the presence of sodium carbonate buffer (brought to pH 6 after gradual addition of 1 mM HCl). Equimolar amounts of EDC and NHS (4 mmol) were added to 20 mL of phosphate-buffered saline (PBS) and were stirred for 20 min at room temperature and then were preincubated at 0 °C for 10 min. To this homogeneous solution, around 80 mg of RhoB was added and magnetically stirred for 2 h. After this, the bPEI solution was added dropwise to this reaction mixture. The reaction mixture was stirred at room temperature for 48 h to allow completion of reaction. The final reaction mixture obtained was then dialyzed (MWCO, 12 kDa) against deionized water for 3 days until a constant fluorescence was observed in dialyzing medium. The resultant RhoB−bPEI conjugate retained within the dialysis tube was then freeze-dried and then was diluted to working concentrations in deionized water.

Synthesis of RBP Polyplexes. RhoB−bPEI-pDNA (plasmid DNA) (RBP) complexes with different N/P ratios were synthesized by adding appropriate volumes of RhoB tagged bPEI to an equivalent amount of pDNA in deionized water. The pDNA and RhoB tagged bPEI mixture was gently mixed and then was incubated at room temperature for 20−30 min to facilitate complete interaction.

DOI: 10.1021/acsami.5b05280
ACS Appl. Mater. Interfaces 2015, 7, 18717−18731

DNA Binding Assay. The encapsulation efficiency and stability of polyplexes formed between RhoB modified bPEI and pVITRO2-GFP/CD::UPRT plasmid was evaluated by gel retardation assay at different weight ratios. Different volumes of pDNA (0.4 mg/mL) were added to RhoB modified bPEI (1 mg/mL) in PBS. The mixture was then vortexed for 5 s and then was allowed to stand for 10 min at room temperature in order to facilitate efficient encapsulation. The total amount of DNA was kept constant with varying bPEI concentration in each reaction mixture so as to attain different N/P ratios. Thus, formed DNA-bPEI polyplexes were then loaded in 0.8% (w/v) agarose gel and were run at 65 mV for 45 min. The DNA bands were then monitored under UV illumination by BioRad gel documentation system at appropriate exposure time.

DNase I Protection Assay. The RhoB tagged bPEI ability to circumvent predisposal of encapsulated pDNA to cellular nuclease was assayed by DNase I protection assay. RBP complexes with the same N/P ratios as adapted during encapsulation studies (each with 500 μg of pDNA) were treated with 0.6 U DNase I for 15 min at 37 °C. After the incubation period, the reaction was terminated by addition of 1.5 mL of ethylenediaminetetraacetic acid (EDTA) (50 mM) followed by inactivation of DNase I enzyme at 65 °C for 15 min. To confirm the intactness of pDNA within the complexes, the encapsulated pDNA was released from the RhoB−bPEI complexes by addition of 3 mL of 4 mg/mL heparin which competitively binds with pDNA. The reaction mixture was allowed to stand at 37 °C for 3 h to ensure complete dissociation of complexes. The pDNA thus released was then assessed by gel electrophoresis (0.8% agarose) at 65 V for 1 h. Bare pDNA processed through identical steps was adapted as experimental control.

Size, Zeta Potential, and Morphology of RBP Complexes. The hydrodynamic radius and surface charge of RBP complexes at optimum N/P ratio was estimated by Malvern Zetasizer Nano ZS90 (Malvern, U.K.) at 25 °C. All data were acquired in monomodal acquisition mode as per Smoluchowski theory. The morphology of RBP complexes was examined by atomic force microscope (AFM-NTEGRA PNL) with Si cantilever (spring constant, 21 N/m) probes operating in semicontact mode at a resonance frequency of 160 kHz. The images were acquired with scan field of 5 μm × 5 μm and then were processed further using NOVA software for size and roughness analysis.

Fabrication of RBP/5-FC Loaded Core−Shell Nanofibers. Standard core−shell electrospinning apparatus procured from ESPIN Nano (Physics Equipment and Company, India) was used for fabrication of core−shell nanofibers. The presynthesized RBP polyplexes (10 mL of RBP at N/P ratio of 3) were concentrated initially by dialysis and then were dissolved in 3.5 wt % PEO and 0.8 wt % bPEI solution in distilled water. After curing the solution for 3−4 h, the polymer blend was fed as shell solution in the electrospinning apparatus. The prodrug 5-FC (0.25 wt %) was added to 3.5 wt % PEO and 1% bPEI in distilled water and was fed as core solution in the electrospinning setup. The coaxial spinneret of electrospinning unit comprised of a 10 gauge inner needle was concentrically positioned within an outer needle of 20 gauge diameter. The solutions were fed into vertical coaxial electrospinning apparatus with two independent programmable peristaltic microsyringe pumps. The spinneret tip was connected to a variable high voltage power supply to dissipate charge into the polymer solution. The instrument was operated at 14 kV. The flow rate for core and shell drug−polymer blend was maintained at 0.15 mL/h and 0.2 mL/h, respectively. The nanofiber produced in the process was collected over grounded stationary metal collector positioned at a distance of 20 cm from the spinneret. The nanofiber deposition was carried out for a stipulated time under a controlled cabinet temperature of 32 °C and a constant relative humidity of 55%.

Cross-Linking of Core−Shell Nanofibers. The RBP complex and 5-FC loaded core−shell nanofibers were pretreated with gluteraldehyde (50% v/v) vapor for 10 s in a closed chamber at 40 °C. After gluteraldehyde vapor treatment, the fibers were transferred to a hot air oven at 45 °C for 3 h to remove the remnant unreacted gluteraldehyde from the scaffold. The cross-linked core−shell nanofiber was then UV sterilized for 20 min before being carried over for cell culture studies.

Characterization of Core−Shell Nanofiber. The morphology of 5-FC and RBP complex loaded core−shell nanofiber was observed by Ultra plus-Carl Zeiss field emission-scanning electron microscope (FE-SEM) operating at 5 kV. The fibers were gold coated for 30 s in Denton gold sputter unit before being mounted in FE-SEM. The core−shell nanofiber images were procured and then were further processed by ImageJ software to obtain the mean fiber diameter and fiber diameter distribution. The 5-FC entrapment efficiency was calculated by the following equation:

$$\text{entrapment efficiency} = (\text{total mass of drug released from nanofiber} / \text{mass of total drug added}) \times 100$$

The total amount of 5-FC loaded in core−shell nanofiber was estimated by disrupting the drug-loaded nanofibers in PBS by probe sonication for 10 min (2 s on and 3 s off). After complete disruption of nanofiber, 5-FC was released into PBS which was later quantified with respect to 5-FC standard plot to arrive at total mass of 5-FC loaded. The degree of swelling and weight loss of core−shell nanofiber when incubated in PBS was estimated by the following equation:

$$\text{degree of swelling}\%(W_S) = (W_1 - W_2)/W_2 \times 100$$

$$\text{weight loss}\%(W_L) = (W_2 - W_3)/W_2 \times 100$$

where W_1 is the weight of the swollen nanofiber, W_2 is the initial weight of the sample before incubation, and W_3 is the weight of the PBS incubated sample after drying at 40 °C.

RBP polyplexes and 5-FC loaded core−shell nanofibers were cross-linked in the presence of gluteraldehyde vapor and were then soaked in PBS (pH 7.2) at 37 °C for 48 h. After the stipulated incubation period, the wet and dry masses of nanofibers were estimated in order to determine the degree of swelling and weight loss.

Drop Shape Analysis System-DSA30 (Kruss, Hamburg, Germany) was used to measure static contact angles sessile drop method. In brief, around 30 μL of ultrapure water was dropped onto 5-FC and RBP polyplexes loaded core−shell PEO-bPEI nanofiber surface, and the contact angle was calculated after 60 s time span.

The Fourier transform infrared (FTIR) spectra of core−shell nanofibers with different compositions were acquired by Thermo Nicolet spectrometer using KBr pellets in the range 4000−400 cm^{-1}. FTIR spectra of control samples were also

DOI: 10.1021/acsami.5b05280
ACS Appl. Mater. Interfaces 2015, 7, 18717−18731

acquired for foolproof interpretation of peaks. TG-DTA analysis of core−shell nanofibers was carried out to assess its composition and stability. About 10 mg of sample was heated from 32 to 550 °C at a constant rate of 10 °C/min in nitrogen atmosphere by EXSTAR TG/DTA 6300.

Release Study of RBP Complex and 5-FC from Core−Shell Nanofibers. RBP and 5-FC loaded core−shell nanofibers (15 mg) were immersed in 5 mL PBS (pH 7.0) for 96 h under static conditions. At each time point, around 100 μL of release medium was transferred to fresh wells for UV−vis absorbance spectroscopic and fluorescence spectroscopic analysis. The release medium withdrawn at each time point was then replenished with an equivalent amount of fresh medium. Time-dependent release of RhoB tagged bPEI-pDNA complexes was monitored by a corresponding increase in florescence (associated with RhoB) in the release medium. An excitation wavelength of 510 nm was used, and emission spectra were acquired from 540 to 700 nm with an interval of 5 nm by Cytation3 multimode reader (Biotek Instruments, Inc.). The obtained fluorescence maximum value at 565 nm was normalized with respect to fluorescence values obtained for uncross-linked RBP and 5-FC loaded core−shell nanofiber to arrive at percentage release of complex. Corresponding 5-FC release with respect to time was quantified by acquiring absorbance at 276 nm by UV−vis spectrophotometer and by correlating it to standard plot. All samples in the experiment were in triplicates. The results were represented in terms of cumulative percentage drug release.

$$\text{cumulative percentage of 5-FC released} = M_t/M_\infty \times 100$$

where M_t is mass of 5-FC released at time t and M_∞ is total mass of 5-FC loaded in the nanofiber.

pH Dependent Fluorescence Stability of RBP Complexes. The pH dependent fluorescence stability of RhoB tagged to bPEI in pDNA polyplexes was quantified at different pHs (pH 1−11) by Cytation3 multimode reader (Biotek Instruments, Inc.). The polyplexes were excited with 510 nm laser, and subsequent emission spectra were acquired starting from 540 to 700 nm with intervals of 5 nm.

RBP Uptake Studies. Owing to fluorescence properties of RhoB tagged to bPEI-pDNA polyplexes, its cellular uptake was monitored in real-time basis by fluorescence microscopy (EVOS FL Color, AMEFC 4300). Around 1×10^5 A549 cells were seeded over RBP and 5-FC loaded core−shell PEO nanofibers in three separate wells. Each well was terminated at different time points (i.e., 4, 12, and 16 h) and then was monitored under a fluorescence microscope in order to observe time-dependent cellular uptake and localization of RBP polyplexes. After the destined time span of incubation, the spent media was aspirated from the wells and was replaced with 2 mL PBS containing 2 μL of Hoechst 33342 (stock, 10 mg/mL) and 5 μL Lysotracker green (stock, 50 mM). The cells were incubated at 37 °C for 30 min for proper uptake of dyes and then were fixed by 2% gluteraldehyde solution for 5 min. After gluteraldehyde, fixation cells were monitored under fluorescence microscope using DAPI filter (Hoechst 33342 stained nucleus), green filter (Lysotracker green stained lysosomes), and red filter (RhoB labeled bPEI-pDNA polyplexes).

Time-Dependent Transfection of Suicide Gene (GFP/CD::UPRT). The fraction of A549 cells transfected with GFP/CD::UPRT suicide gene at different time points were initially observed under fluorescence microscope (EVOS FL Color, AMEFC 4300) and were further quantified by flow cytometry (Amnis Flowsight). Around 1×10^5 A549 cells were seeded over RBP loaded core−shell nanofibers in a six-well plate. At 20, 28, 34, and 48 h, the media in the respective wells was removed and replaced with 2 mL PBS containing 1 μL of Hoechst 33342 (10 mg/mL) and was incubated for 5 min. After incubation time, the excess stain was washed with fresh PBS and then was visualized under a fluorescence microscope. Images were acquired under DAPI filter (Hoechst 33342 stained nucleus) and green filter (autofluorescent core−shell nanofibers) and were processed further to generate overlay of two images. After microscopic observation, the same batch of cells was trypsinized and resuspended in PBS for quantification of transfected cells by flow cytometry. The GFP/CD::UPRT expressing green fluorescent transfected cells were distinguished from untransfected cells by exciting green fluorescent protein by 488 nm laser. A plot of normalized frequency % with green fluorescence intensity in channel 2 (Intensity_MC_Ch02) was generated after acquiring 10 000 events for each sample.

Suicide Gene Bystander Effects. To assess the bystander effects of CD::UPRT suicide gene therapy, a combination of propidium iodide and Hoechst 33342 stain was adapted. A549 cells pretreated with RBP and 5-FC loaded core−shell nanofibers were withdrawn from culture condition at 48, 72, and 96 h and were stained with Hoechst 33342 (1 μL from 10 mg/mL stock) and PI (10 μL from 1 mg/mL stock) in PBS. The cells were incubated at 37 °C for 30 min after which the excess stain was gently washed away with PBS. Images were acquired under DAPI filter, green filter, and red filter and then were overlaid to identify dead, live, transfected, and non-transfected cells.

Cell Viability Assay. Cell lines A549 and L-132 were obtained from the cell repository of National Centre for Cell Science, India. Cells were maintained in DMEM (high glucose) medium supplemented with 10% FBS, 50 U/mL penicillin, and 50 mg/mL streptomycin in a humidified atmosphere in 5% CO_2 at 37 °C. The core−shell nanofibers' ability to deliver suicide gene to cancer cells and subsequently to mediate catabolic conversion of prodrug 5-FC into toxic byproducts was assessed initially by cell viability (MTT) assay as mentioned elsewhere.[10]

Two different concentrations of 5-FC (0.25 and 0.5 wt %) and RBP were loaded in core−shell nanofibers in order to generate four different versions of core−shell nanofibers. Core−shell NF1 and core−shell NF2 were loaded with the same extent of RBP polyplexes in the shell but with 0.25 and 0.5 wt % of 5-FC in the respective nanofiber core. Similarly, core−shell NF3 and core−shell NF4 were loaded with different amounts of RBP polyplexes in the shell but with the same amount of 5-FC (i.e., 0.25 wt %).

Semi-Quantitative Reverse Transcription Polymerase Chain Reaction (RT-PCR). Suicide gene transfection and its subsequent expression by A549 cells were estimated by semiquantitative RT-PCR. Furthermore, the differential expression of apoptotic genes that arises in later stages of suicide gene therapy was also monitored by RT-PCR. The total RNA was extracted from A549 cells subjected to suicide gene therapy at predestined treatment duration by Tri reagent (Sigma-Aldrich, USA). The cDNA was generated by reverse transcription of 3 μg of total denatured RNA using M-MLV reverse transcriptase (Sigma, USA). The cDNA product was used for gene-specific amplification of GFP/CD::UPRT and other

DOI: 10.1021/acsami.5b05280
ACS Appl. Mater. Interfaces 2015, 7, 18717−18731

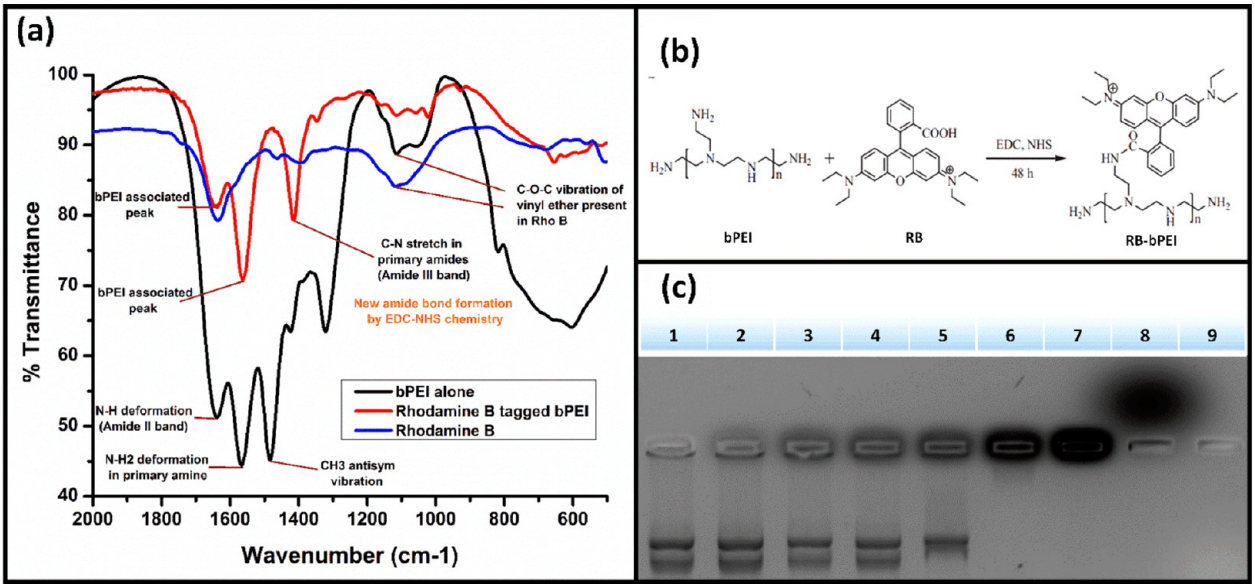

Figure 1. RhoB-bPEI synthesis (a) FTIR spectroscopy and (b) schematic, (c) gel retardation assay of RhoB tagged bPEI-pDNA polyplexes (lane 1, bare pVITRO2-GFP/CD::UPRT plasmid; lane 2, lane 3, lane 4, lane 5, and lane 6 loaded with RBP polyplexes of N/P ratios of 0.5, 1, 1.5, 2, and 3, respectively; lane 7, bare RhoB tagged bPEI; lane 8, RhoB alone; and lane 9, bPEI alone).

apoptotic genes. The forward and reverse primers utilized for PCR amplification are mentioned in Table S1. Beta-actin (housekeeping gene) was adapted as an internal control. The PCR products were finally resolved in 1% agarose gel and were visualized by ethidium bromide staining under UV light. The difference in gene expression was computed from the gene-specific bands obtained by Image lab 4.0 software. The apoptotic genes considered for gene expression studies include bad, bak, bax, p53, caspase-3, and C-myc; apart from these, antiapoptotic genes bcl-2 and bcl-XL were also included in the study.

Flow Cytometry Analysis of Suicide Gene Therapy. The cascade of events that fosters GDEPT was assessed by flow cytometry at different time points. A549 (1×10^5 cells) cells were seeded over RBP and 5-FC loaded core−shell nanofibers and were analyzed at 24, 36, and 72 h. After the respective incubation period, cells were trypsinized and resuspended in PBS (200 μL); to each of the samples, 10 μL of PI was added, and then the cells were incubated at 37 °C for 20 min. The samples were loaded in flow cytometry (Amnis Flowsight), and upon excitation by 488 nm laser, green fluorescence of transfected cells and red fluorescence of PI stained dead cells could be observed in different channels. Around 10 000 events were acquired for each sample and then were analyzed by Amnis Ideas software to arrive at percentage transfected cells and dead cells at different time points.

FE-SEM Analysis of Cellular Morphology. The release of RBP polyplexes from nanofibers and its attachment over cell surface was observed by FE-SEM during the initial period of incubation. Apart from this, subsequent morphological changes manifested by A549 cells seeded over RBP and 5-FC loaded core−shell PEO nanofibers were also clearly discerned under FE-SEM. Treated A549 cells over nanofiberous scaffold were given mild PBS wash and then were fixed with 2% glutaraldehyde solution for 5 min. The remnant glutaraldehyde was washed away by ethanol/water gradient and then was air-dried for 5 min before being observed under FE-SEM.

3. RESULTS AND DISCUSSION

3.1. Synthesis of RhoB Tagged bPEI-pDNA Polyplexes. The efficient conjugation of RhoB to bPEI by EDC/NHS chemistry was confirmed by FTIR and gel retardation assay. During the course of reaction, − COOH groups of the RhoB were covalently bonded to − NH_2 (primary amine) groups of bPEI by amide bonds. A reaction scheme for this process is depicted in Figure 1b. The FTIR spectra of bPEI had peaks at 1481 cm^{-1} (corresponding to antisymmetric stretch of CH_2 in aliphatic compounds) and sharp peaks at 1567 and 1637 cm^{-1} ascribed to N−H deformation in primary amines and amide II band, respectively (Figure 1a). IR spectra of RhoB possessed a characteristic absorption peak at 1630 cm^{-1} corresponding to C═N stretch vibration and another peak at 1467 cm^{-1} corresponding to the presence of benzene rings (ring stretch vibration).[11] FTIR spectra of RhoB tagged bPEI possessed characteristic peaks of bPEI (1567 and 1637 cm^{-1}) and RhoB (1114 and 1087 cm^{-1}). Apart from these, an additional strong peak at 1413 cm^{-1} was observed in RhoB tagged bPEI, which arises because of C−N stretch of primary amides (amide III band) that was formed by EDC-NHS coupled reaction between COOH group of RhoB and terminal NH_2 group of bPEI.

Apart from FTIR analysis, RhoB conjugated bPEI synthesis was confirmed further by gel retardation assay, as RhoB presence could also be monitored under UV. During agarose gel electrophoresis, free RhoB migrates toward the anode (lane 8) under the influence of external field whereas RhoB conjugated to bPEI was retained in the loading well itself (lane 7) (Figure 1c). The higher molecular weight and hyperbranched structure of bPEI limit its mobility during electrophoresis, and as a consequence, RhoB conjugated to bPEI was also retained in the well. A concentration-dependent increase in RhoB-bPEI intensity was also observed in subsequent wells with increasing N/P ratio (lanes 1−6) (Figure 1c). At N/P ratio of 7, pDNA was completely condensed to form stable polyplexes wherein DNA's negative charge was completely masked by amine groups of bPEI

DOI: 10.1021/acsami.5b05280
ACS Appl. Mater. Interfaces 2015, 7, 18717−18731

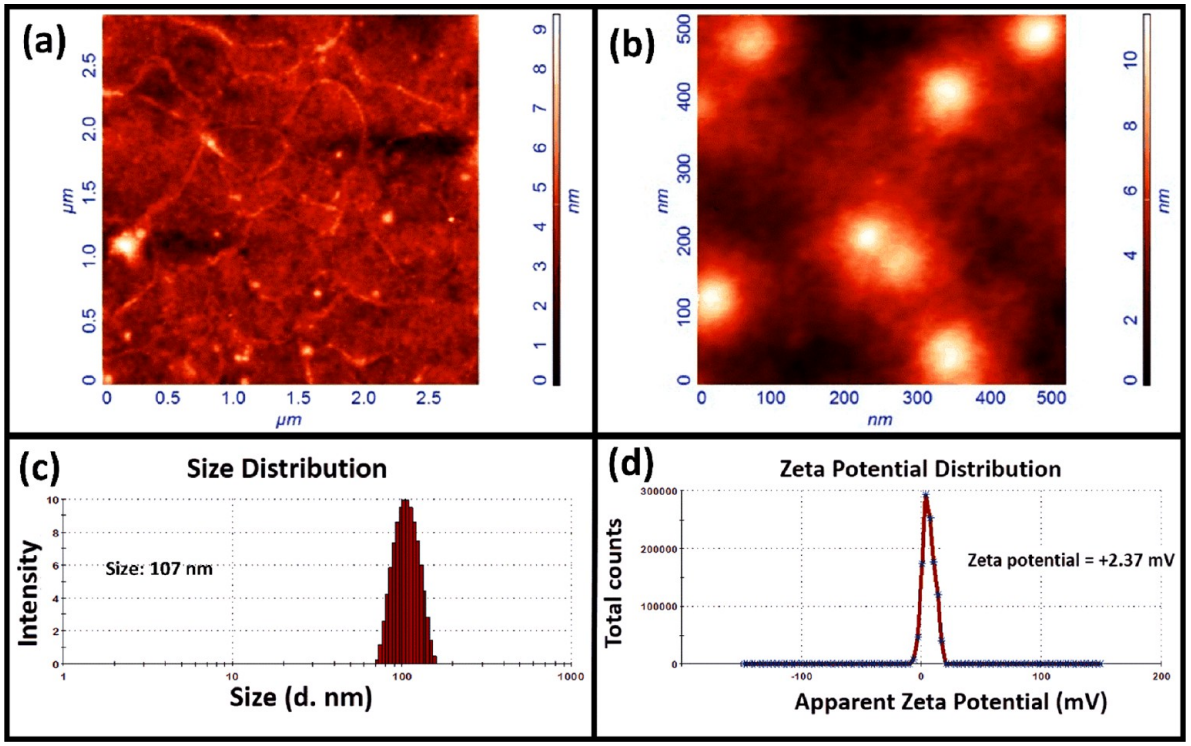

Figure 2. AFM image of (a) pVITRO2-GFP/CD::UPRT plasmid and (b) RBP polyplexes. (c) Size distribution and (d) zeta potential of RBP polyplexes.

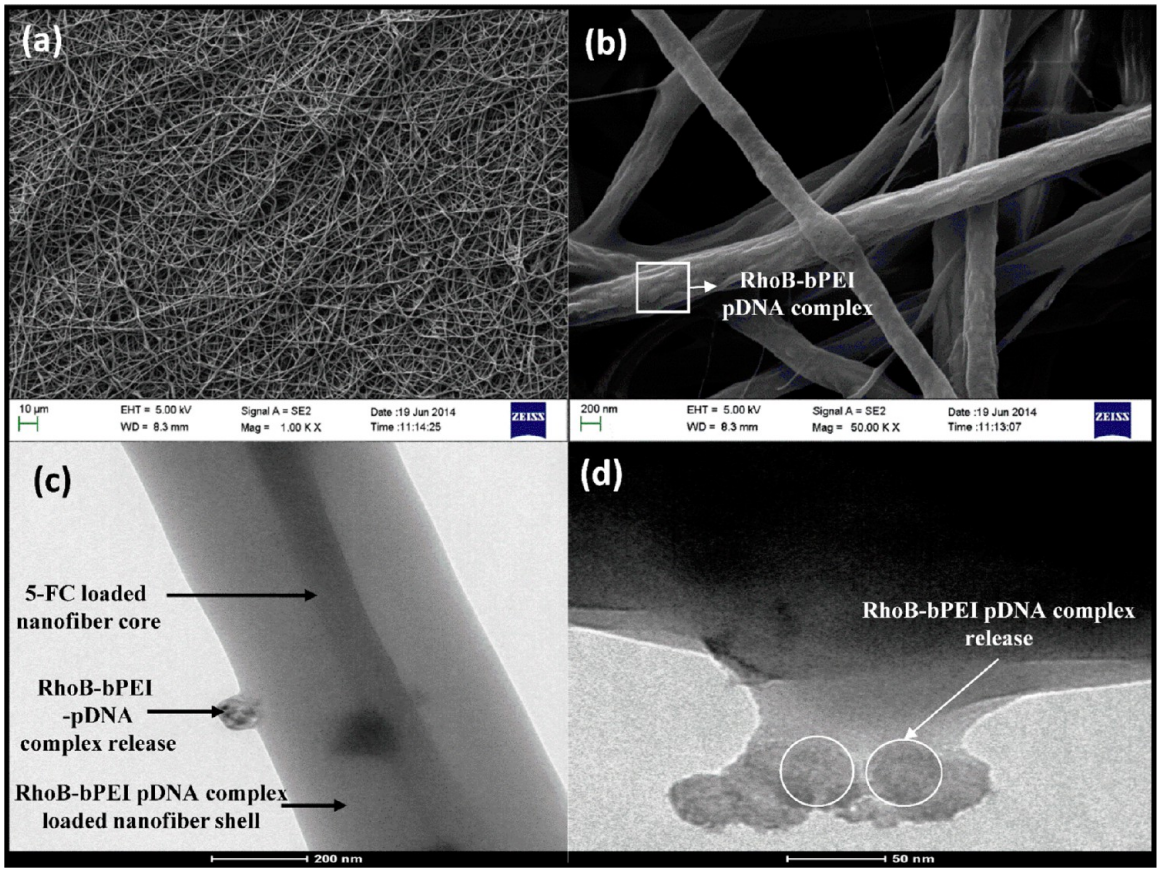

Figure 3. FE-SEM image of RBP and 5-FC loaded core−shell nanofibers (a) at lower magnification to depict uniform fiber distribution, (b) at higher magnification in order to visualize partial demarcation of RBP polyplexes on the surface; (c) TEM images of core−shell nanofibers showing intact core−shell morphology and (d) gradual release of RBP polyplexes from nanofibers.

DOI: 10.1021/acsami.5b05280
ACS Appl. Mater. Interfaces 2015, 7, 18717−18731

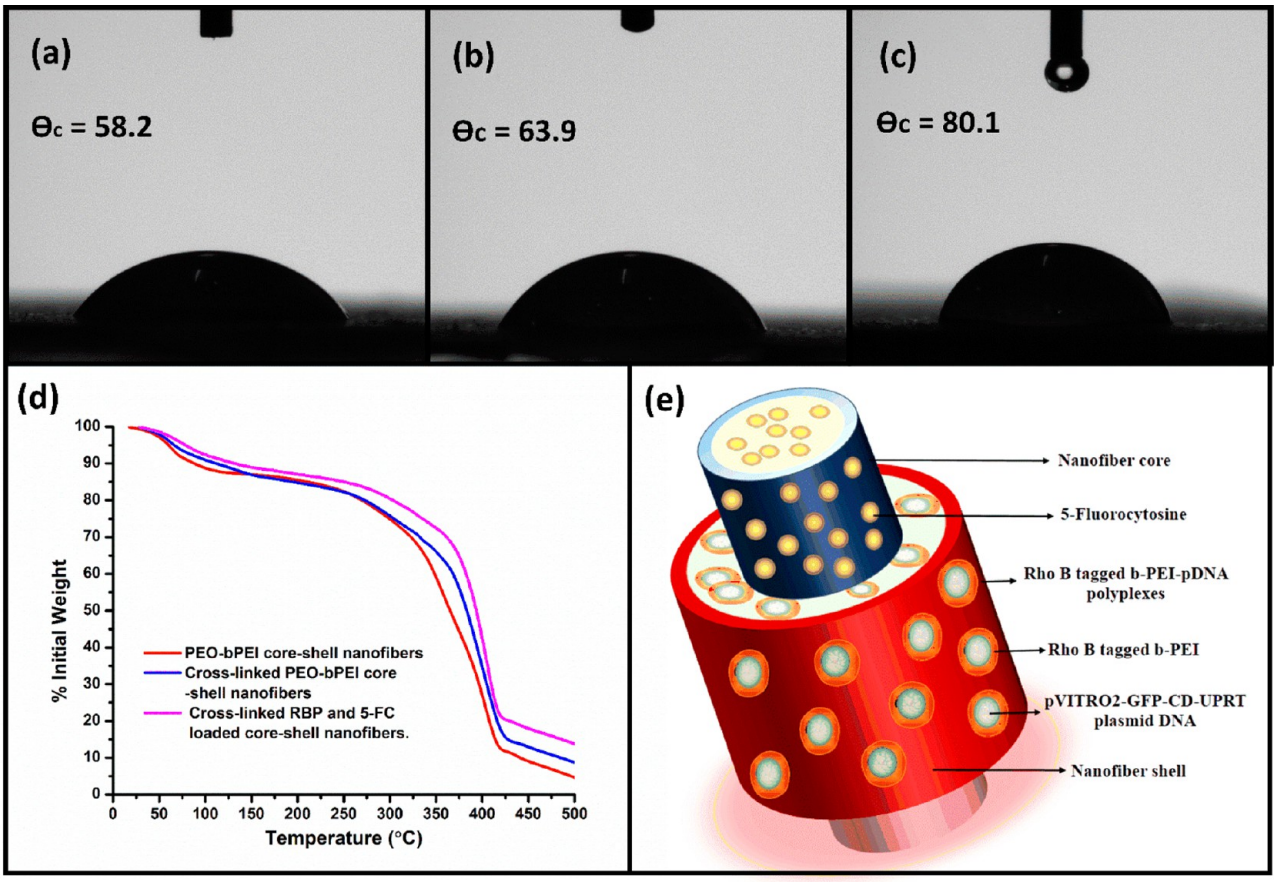

Figure 4. Water contact angle measurement for (a) bare PEO-bPEI core−shell nanofibers, (b) RBP polyplexes and 5-FC loaded core−shell nanofibers, and (c) gluteraldehyde cross-linked core−shell nanofibers loaded with RBP polyplexes and 5-FC; (d) TGA of different versions of core−shell nanofibers; (e) illustration of core−shell nanofibers loaded with RBP polyplexes and 5-FC.

because these polyplexes were retained in loading wells even under applied external field. The atomic force microscopy (AFM) of RBP polyplexes (N/P ratio 7) indicated condensed complexes of uniform size distribution in the range of 78−90 nm (Figure 2b). Furthermore, the integrity of plasmid DNA released from RBP polyplexes was also established by AFM (Figure 2a). Thus, formed RBP complexes were distinct with minimal intercomplex interaction which suggests better stability and intactness of polyplexes. The hydrodynamic size distribution of RBP polyplexes was estimated to be ∼107 nm (mean diameter) by dynamic light scattering (DLS) measurement which was in coherence with AFM images (Figure 2c). The polyplexes' zeta potential in aqueous solution was estimated to be +2.37 mV owing to excessive free amine groups of bPEI present on its surface. RhoB tagged to bPEI moieties is also positively charged, and thus, it contributes partially to positive zeta potential of the polyplexes (Figure 2d). Bare bPEI polyplexes with pDNA at the same N/P ratio (i.e., 7) were observed to have marginally higher zeta potential of 3.15 mV as few amine groups of bPEI were consumed in amide bond formation during RhoB conjugation. The integrity of pDNA in the RBP polyplexes on predisposal to intracellular DNase enzymes was confirmed by DNase I protection assay (Figure S1). The lane 1 indicates control plasmid at the same concentration as used for encapsulation followed by negative control where free DNA is completely degraded by DNase I. In subsequent lanes, that is, lanes 3−5, bands corresponding to intact plasmid present within RBP polyplexes were observed. The increasing plasmid intensity with higher fraction of bPEI in RBP polyplexes clearly indicates that a higher proportion of bPEI could effectively mask a greater fraction of pDNA from DNase I mediated degradation.

3.2. Characterization of Core−Shell Nanofibers Loaded with RBP Polyplexes and 5-FC. The FE-SEM observation of electrospun core−shell PEO nanofibers loaded with RBP and 5-FC indicated uniform fiber diameter distribution of 350 ± 58 nm (Figure 3a). Core−shell nanofiber images at higher magnification under FE-SEM revealed partial demarcation of spherical RBP polyplexes present in the nanofiber shell layer (Figure 3b). As distinctly visible under FE-SEM, these polyplexes were incorporated uniformly within nanofibers and remained intact in shape and morphology even after electrospinning. The core−shell morphology of nanofibers could be discerned clearly under TEM wherein the nanofiber core loaded with 5-FC generated a clear contrast with the shell layer loaded with RBP polyplexes (Figure 3c). The TEM image of RBP and 5-FC loaded core−shell nanofiber in Figure 3c, d indicates the event of polymer dissolution from the nanofiber shell layer and gradual elution of RBP polyplexes from the nanofibers during the initial phase of PBS incubation. Prodrug 5-FC loaded within the nanofiber core remains intact with minimal diffusion during the initial phase. This time lag attained between release of two components (i.e., RBP and 5-FC) is considered favorable for fostering efficient suicide gene therapy.[13] Postfabrication cross-linking of core−shell nanofibers with gluteraldehyde limits dissolution of RBP to a great extent.

DOI: 10.1021/acsami.5b05280
ACS Appl. Mater. Interfaces 2015, 7, 18717−18731

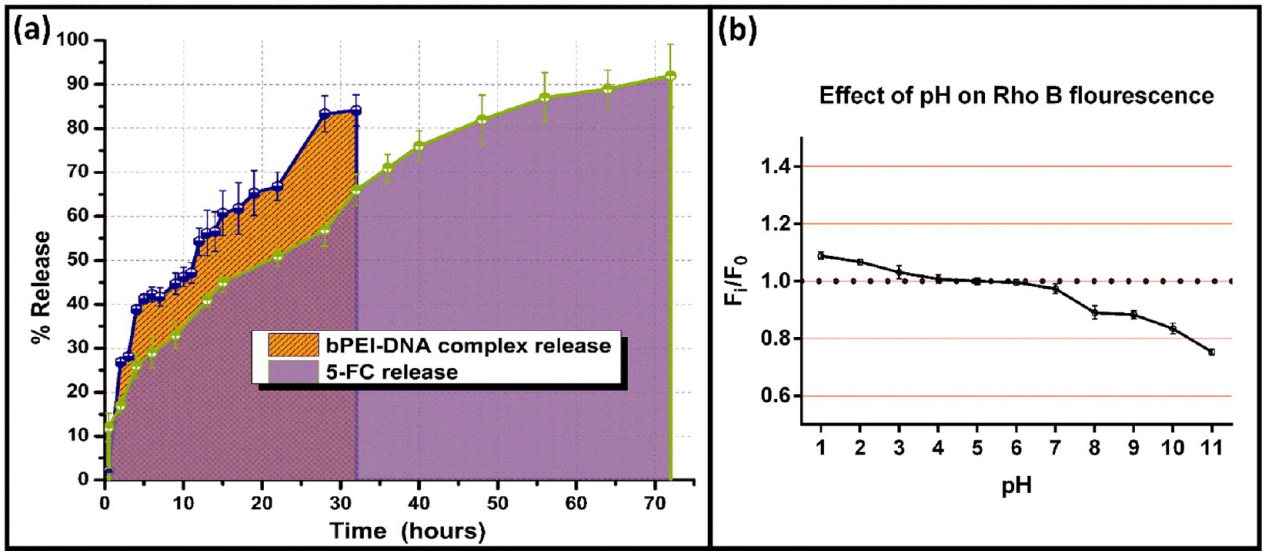

Figure 5. (a) Release profile of RBP polyplexes and 5-FC from core−shell nanofibers; (b) effect of pH on RhoB fluorescence.

The presence of a small fraction of primary amines on the surface of RBP extends a possibility of generating cross-links with free bPEI present in the matrix of the nanofiber.[14] The presence of such cross-links may at times strip off a small fraction of bPEI during the course of RBP dissolution and thereby reduce the polyplex diameter to a certain extent as observed in Figure 3d. The presence of such cross-links also leads to extrusion of the polymer matrix along with dissoluting RBP into the release medium (Figure 3d).

Core−shell nanofibers being hydrophilic in nature tend to exhibit polymer swelling and dissolution with respect to time of incubation in hydrophilic environment. The degree of cross-linking determines polymer swelling and dissolution. This hypothesis was confirmed when core−shell nanofibers with higher bPEI content (i.e., 1.2 wt %) were observed to undergo lower weight loss (i.e., 26.1%) and polymer swelling (i.e., 31.7%) as compared to core−shell nanofibers with lower bPEI content (i.e., 0.8 wt %) for which weight loss and polymer swelling was estimated to be 33.4% and 37.3%, respectively.

Contact angle analysis of core−shell nanofibers clearly depicted their hydrophilic nature (contact angle < 90°) owing to the presence of hydrophilic components PEO and bPEI (Figure 4a−c). The bare core−shell nanofibers possessed a contact angle value of 58.2° which increases slightly to 63.9° upon loading with RBP and 5-FC in core and shell of the nanofibers, respectively. Subsequently, partial gluteraldehyde mediated cross-linking of nanofibers imparts it better stability in a hydrophilic environment which led to a corresponding increase in the contact angle value to 80.1°. The cross-linked nanofibers being stable in hydrophilic environment could retain water which also contributes to an increase in the contact angle values.

The effect of cross-linking and drug loading on thermal stability of core−shell nanofibers was assessed by thermal gravimetric analysis (Figure 4d). The % weight loss of nanofibers with respect to temperature was plotted to distinguish different regimes of polymer and drug degradation. Three different versions of core−shell nanofibers were adapted for this study, that is, un-cross-linked bare PEO-bPEI core−shell nanofibers, cross-linked bare PEO-bPEI core−shell nanofibers, and cross-linked RBP and 5-FC loaded core−shell nanofibers. A common phase of initial mass loss was observed (up to 65 °C) in all three cases which is ascribed to loss of adsorbed moisture content. At higher temperature regimes, cross-linked nanofibers exhibited better thermal stability as compared to its un-cross-linked counterpart. Gluteraldehyde mediated interchain imide cross-links generated between amine groups of bPEI render the core−shell nanofibers thermal stability.[14] A schematic representation of gluteraldehyde mediated bPEI cross-linking is shown in Figure S2. The drastic loss in mass between 255 and 320 °C is said to arise because of thermal decomposition of free amine groups of bPEI moiety. The long hydrocarbon chains of PEO begin to degrade gradually at 350 °C, and subsequent mass loss was observed up to 520 °C in all three cases. The weight loss profile was observed to be uniform throughout without any abrupt fluctuations indicating the uniform distribution of drug and RBP polyplexes in the polymer phase. A schematic representation of RBP polyplex and 5-FC loaded core−shell nanofiber fabricated in this work is provided in Figure 4e.

3.3. Release of RBP Polyplexes and 5-FC from Core−Shell Nanofibers. Simultaneous release of RBP polyplexes and prodrug 5-FC from the nanofiberous scaffold was quantified and represented as percentage release with respect to time (Figure 5a). It was observed that at the end of 32 h, almost 85% of RBP polyplexes loaded in the nanofiber shell was released whereas only 65% of 5-FC loaded in nanofiber core was released in the meantime. The RBP complexes loaded in the nanofiber shell layer were released during the initial phase of incubation followed by controlled and sustained release of 5-FC loaded in the core of the nanofibers. This time lag between release of RBP from the nanofiber shell and 5-FC from the nanofiber core is said to arise because of two different factors, one is their core/shell localization and the other is the extent of cross-linking. The nanofiber core solution was initially supplemented with gluteraldehyde (0.05 vol %) which led to a higher extent of cross-linking in polymer matrix in order to attain a prolonged release of prodrug 5-FC from the nanofibers.[14] Thus, the distinct release profile of RBP polyplexes (i.e., suicide gene) and prodrug is handy in fostering higher therapeutic efficacy of suicide gene therapy. The RBP polyplexes incorporated within the nanofiber shell layer begin

DOI: 10.1021/acsami.5b05280
ACS Appl. Mater. Interfaces 2015, 7, 18717−18731

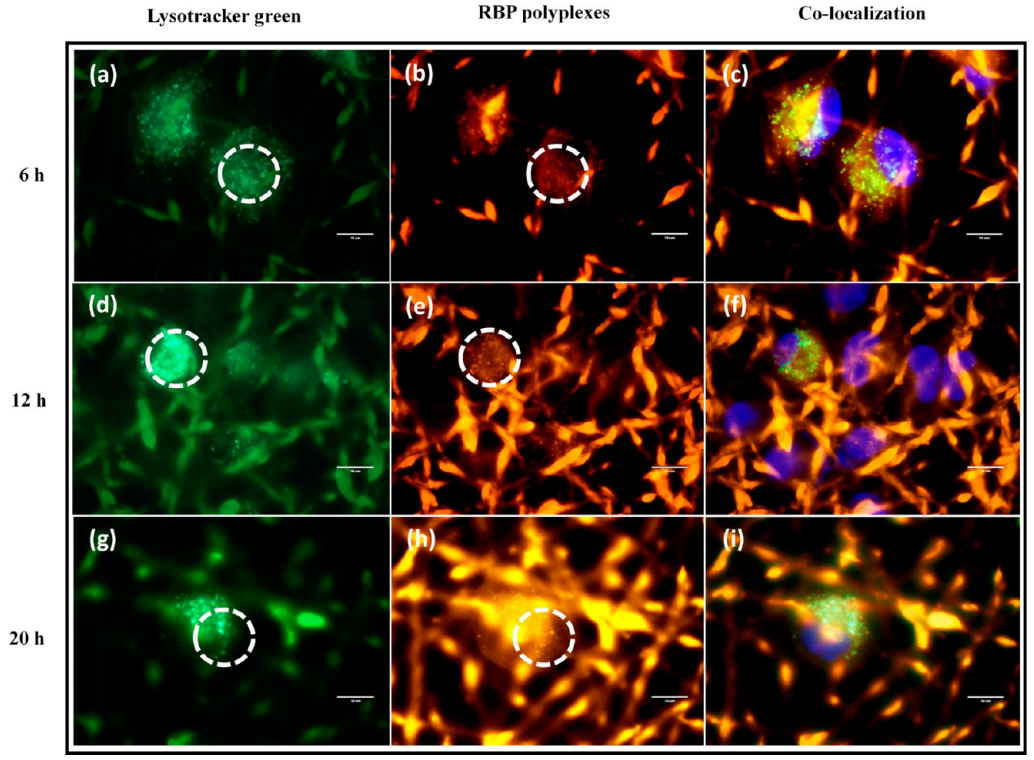

Figure 6. RhoB tagged bPEI-pDNA polyplexes (column 2) colocalization (column 3) within lysotracker green labeled (column 1) lysosomes at 6 h (a–c), 12 h (d–f), and 20 h (g–i).

to surface after gradual dissolution of PEO (Figure 3b). The event of PEO dissolution and subsequent release of RBP in the hydrophilic environment is a dynamic process involving solvent penetration and polymer dissolution at two different fronts. The RBP polyplexes released from the nanofibers were taken up by A549 cells in the vicinity which upon transfection expressed GFP and CD::UPRT genes. These transfected cells expressing the suicide gene were subsequently predisposed to prodrug 5-FC released in the later stages. Almost 91% of 5-FC loaded in the core–shell nanofibers was released by the end of 72 h which was then metabolically converted into toxic byproducts when acted upon by the suicide gene expressed in the transfected cells. At the outset, core–shell nanofiberous scaffold fabricated in the present study could subsequently release RBP polyplexes and 5-FC in a controlled and sustained manner thus extending the scope for eliminating cancer cells by GDEPT.

3.4. pH Dependent Fluorescence Properties of Rho-bPEI Conjugates. RhoB conjugated to bPEI present in the polyplexes serves as a probe to monitor RBP release from the core–shell nanofibers and also aids in tracking its fate following cellular uptake. Previous literature indicates that PEI based carriers end up in highly acidic lysosomes immediately after cellular uptake.[7] Thus, to monitor the intracellular fate of RhoB tagged bPEI-pDNA polyplexes, its fluorescence stability with respect to pH was evaluated. It was observed that with a fall in pH there was considerable increase in fluorescence emission of RhoB and vice versa (at λ_{max} = 575 nm, λ_{exc} = 530 nm). In acidic medium, the amine group of bPEI was completely protonated thereby predisposing tagged RhoB to highly acidic conditions. The dye RhoB was present in a spirocyclic structure which exhibits protonation dependent fluorescence properties.[12] In acidic conditions, the spirocyclic structure of RhoB opened up, which manifests an increase in fluorescence, whereas in basic conditions, it was deprotonated leading to ring closure leading to a corresponding decline in fluorescence (Figure 5b). Thus, fluorescent RhoB-bPEI conjugate system can effectively track intracellular localization of RBP complexes.

3.5. RBP Polyplex Cellular Uptake Studies. Owing to positively charged amine groups (of bPEI) present on the surface of RBP polyplex, they tend to adhere to the cellular membranes after being released from core–shell nanofibers.[15] It was observed that immediately after adherence of RBP polyplexes over a cellular membrane they were internalized into the cells by endosomes. The event of endosome uptake of RBP polyplexes and its fusion with lysosome was monitored in real time by monitoring fluorescent RhoB tagged to RBP polyplexes under a fluorescent microscope (Figure 6b, e, and h). As observed in the overlay of images, during the initial stages of polyplexes uptake, RBP polyplexes were not localized at the same position as the lysotracker green labeled lysosomes (Figure 6c, f, and i) which depicted the event of endosomal uptake. After 12 h, endosomes carrying RBP polyplex were observed to fuse with lysotracker green labeled lysosomes. The colocalization of red fluorescent RhoB in polyplexes with green fluorescent lysosomes confirmed the event of endolysosome fusion. The presence of protonophoric amine groups of bPEI in RBP polyplexes led to acidification of lysosomes which was followed by their lysis by proton sponge effect.[16]

3.6. Transfection of A549 Cells with Suicide Gene in RhoB Labeled bPEI-pDNA Polyplexes. The expression of CD::UPRT suicide gene in transfected A549 cells was monitored by GFP expression under fluorescence microscope in a time-dependent manner. Both nontransfected and transfected cells were stained with Hoechst 33342, whereas only GFP/CD::UPRT transfected cells expressed GFP. The overlay of fluorescent images acquired in DAPI filter and green filter clearly indicated relative fractions of transfected and

DOI: 10.1021/acsami.5b05280
ACS Appl. Mater. Interfaces 2015, 7, 18717–18731

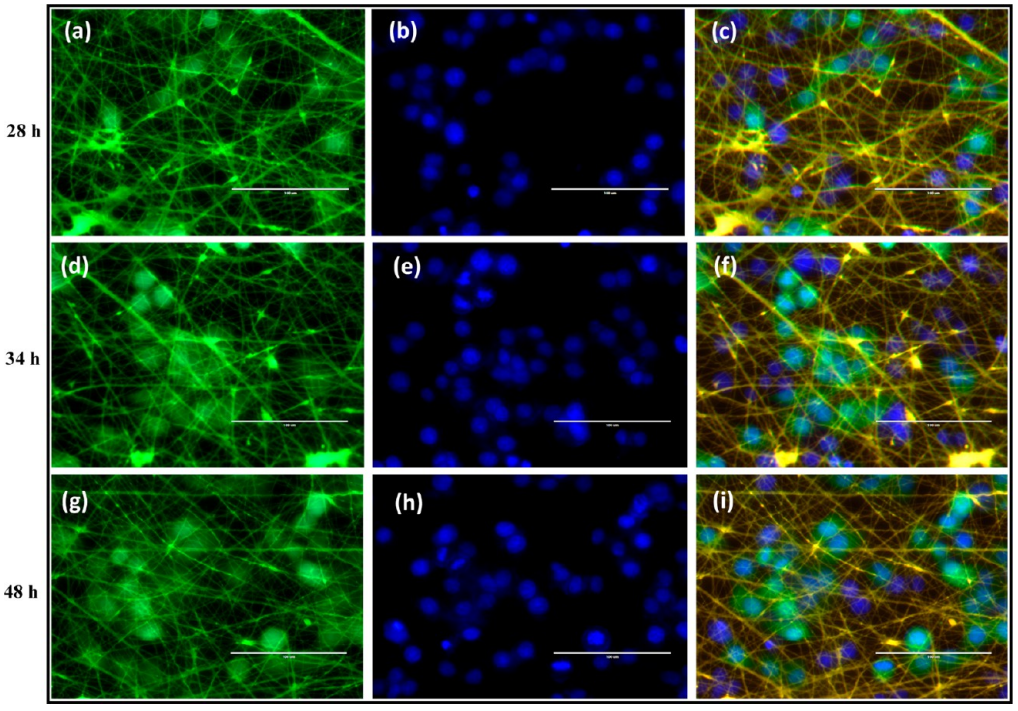

Figure 7. GFP expressing (column 1) suicide gene transfected A549 cells seeded over RBP and 5-FC loaded core−shell nanofibers and Hoechst 33342 labeled live cells (column 2) at (a, b) 28 h; (d, e) 34 h; and (g, h) 48 h. (c, f, i) Overlay of images at respective time points depicts fraction of transfected cells.

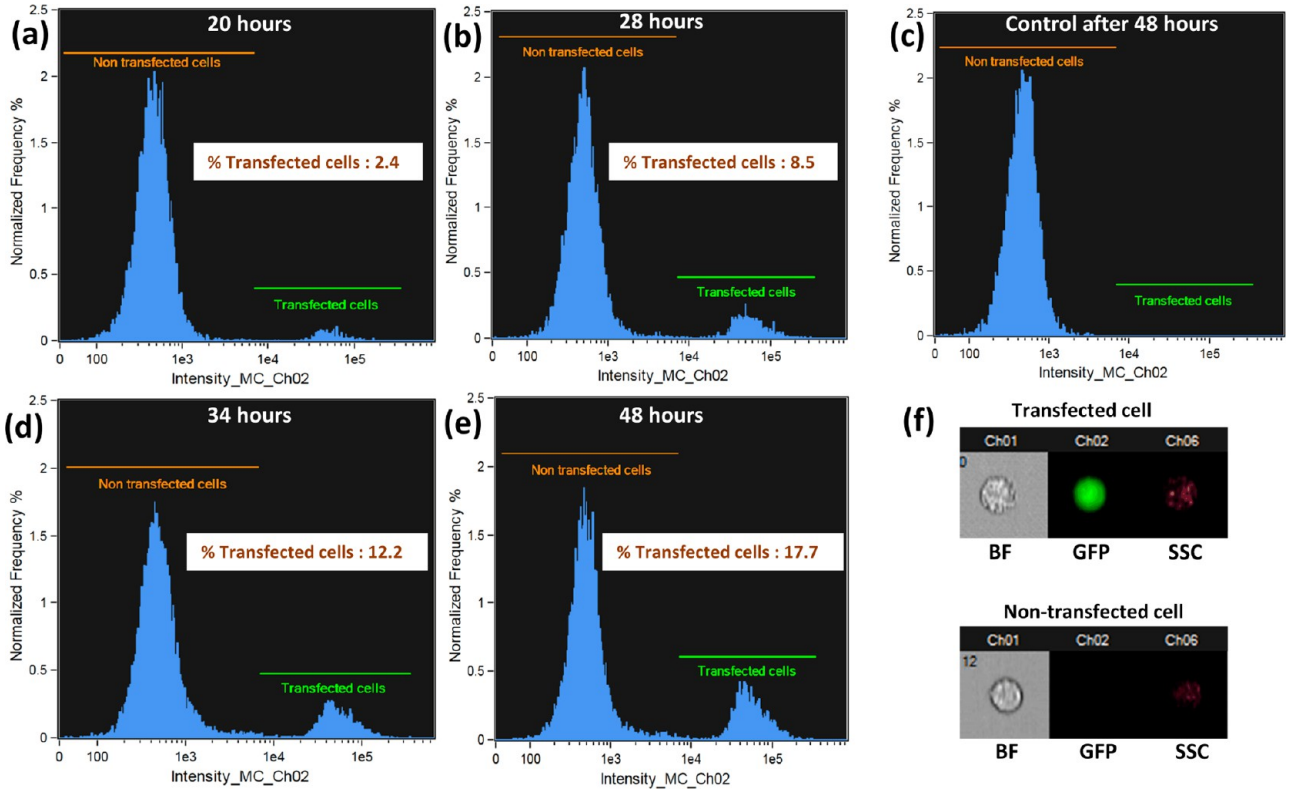

Figure 8. Percentage of A549 cells transfected with GFP/CD::UPRT plasmid after seeding them over RBP and 5-FC loaded core−shell nanofibers at (a) 20 h, (b) 28 h, (d) 34 h, (e) 48 h, and (c) after 48 h seeding over bare core−shell nanofibers; (f) representative images of transfected and nontransfected cells in different channels.

nontransfected cells at different time points. To assess the efficiency of transfection core−shell nanofibers loaded with RBP, polyplexes alone were used in this study. As expected, the relative fraction of A549 cells expressing suicide gene increased with respect to time (Figure 7). To further complement fluorescent microscopic observation, the treated cells were

DOI: 10.1021/acsami.5b05280
ACS Appl. Mater. Interfaces 2015, 7, 18717−18731

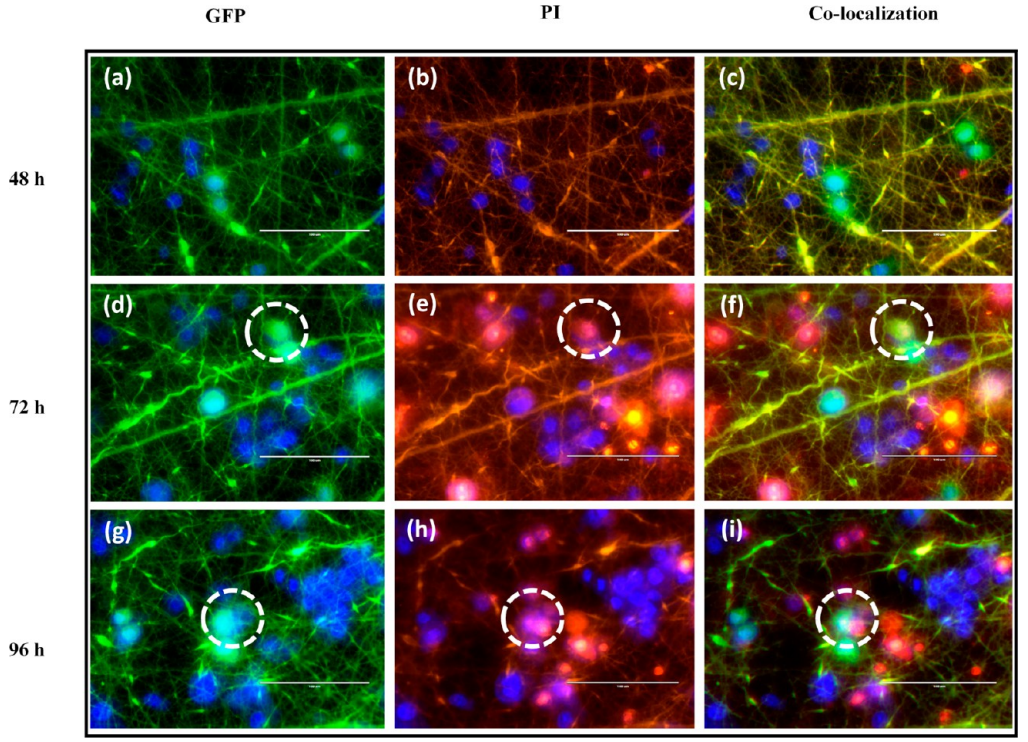

Figure 9. Bystander effects monitored by classifying cell population as (a, d, g) GFP expressing transfected or nontransfected at 48, 72, and 96 h, respectively, and (b, e, h) PI stained dead or live cell. (c, f, i) Overlay of both GFP filter and red filter to identify the dead cells as suicide gene transfected cell or nontransfected.

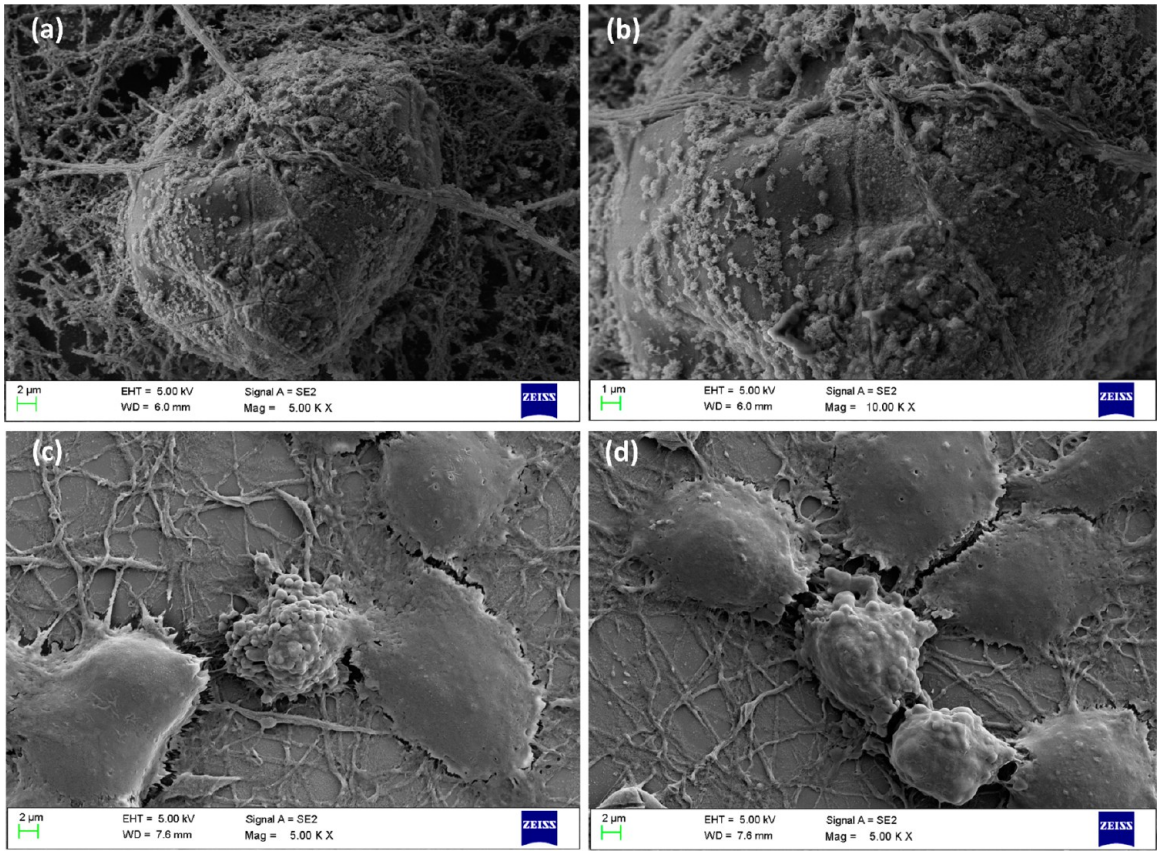

Figure 10. FE-SEM images of A549 cells seeded over core−shell nanofibers indicating events of (a, b) RBP polyplex attachment over A549 cells, (c, d) apoptotic A549 cells at 72 h.

DOI: 10.1021/acsami.5b05280
ACS Appl. Mater. Interfaces 2015, 7, 18717−18731

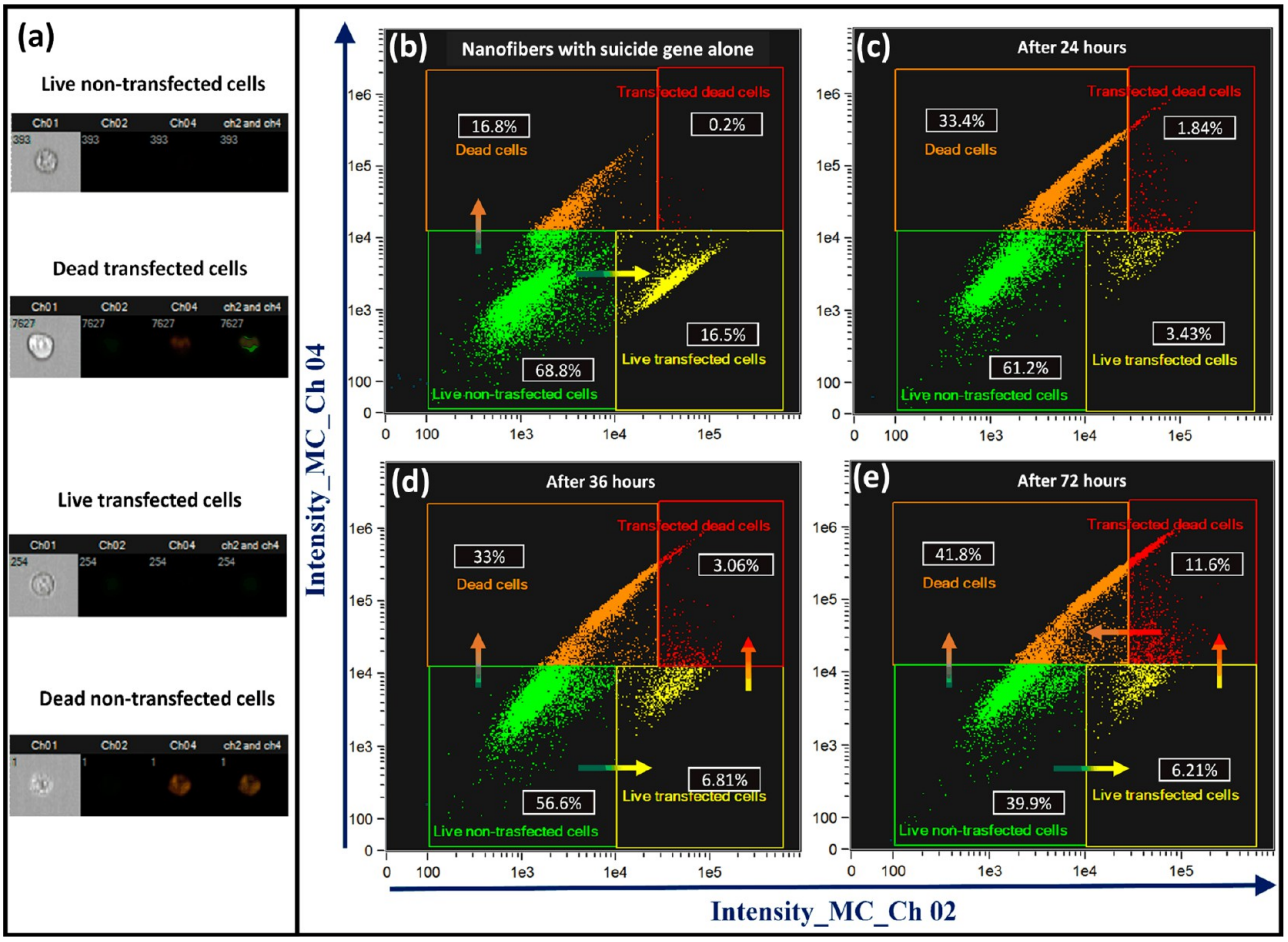

Figure 11. Flow cytometry (a) images of diverse A549 populations as observed in different channels; analysis of A549 cells seeded over (b) control nanofibers with RBP alone at 72 h and (c) core−shell nanofibers loaded with RBP and 5-FC at 24 h, (d) 36 h, (e) 72 h.

analyzed by flow cytometer for GFP expression (% transfected cells) after respective time points (Figure 8). The representative images of A549 cells in each channel for both transfected and nontransfected cells were acquired with appropriate gating of cell population. The transfected cells were monitored by green fluorescence in Ch02, whereas brightfield and side-scattered images were obtained in Ch01 and Ch06. The fraction of transfected cells increased from 2.4% at 20 h to 8.5% at the end of 28 h indicating the significant number of transfected cells appearing after 28 h. A gradual release of RBP from core−shell nanofibers, its uptake, and the event of suicide gene expression by transfected cells account for the delayed GFP expression monitored after 20 h. After 48 h, GFP/CD::UPRT suicide gene expression increased to 17% which is sufficient to convert prodrug 5-FC into toxic metabolites such as 5-FUMP, 5-FdUMP, and 5-FUTP in order to foster host cell apoptosis (expressing suicide gene) and subsequent bystander effects. As observed in the release study, almost 85% of RBP polyplexes were released by the end of 32 h; the percent of transfected cell population plateaued at 17% by the end of 48 h. The time span of CD::UPRT gene delivery, transfection, and expression (i.e., nearly 32 h) clearly suggests that suicide gene's antiproliferative effects against A549 cells will be effectively observed only after 32 h. On the basis of these observations, CD::UPRT suicide gene therapy efficacy was monitored at 48 and 96 h by cell viability assay.

3.7. Bystander Effects of CD::UPRT Suicide Gene Therapy. Apart from inducing apoptosis in the host cell, the antiproliferative metabolites transduced by CD::UPRT enzyme also act upon the cells in the vicinity, thereby mediating the bystander effects. A combination of dyes Hoechst 33342 and PI was used to observe the bystander effects under a fluorescence microscope. The live cell nucleus was stained with Hoechst 33342, whereas the dead cell nucleus was stained with PI alone. The transfected cells expressed GFP which makes them distinctly visible under green filter. In the initial stages (i.e., before 28 h), although transfected cells (GFP/CD::UPRT expressing cells) were observed, no significant number of dead cells (stained with PI) were present (Figure 9a−c). In the later stages, transfected cells expressing CD::UPRT enzyme converted prodrug 5-FC into 5-FU and led to apoptosis of the host cell. Transfected A549 cells expressing CD::UPRT gene underwent apoptosis and were visible under both green filter (GFP expression) and red filter (dead cell nucleus stained with PI) (Figure 9d−f). At the same time point, a few nontransfected dead cells stained with PI were also observed in the vicinity which indicated bystander effects were caused by toxic metabolic intermediates generated by CD::UPRT enzyme (Figure 9g−i). Similar observations were made in FE-SEM imaging of cells, wherein transfected cells underwent membrane blebbing (characteristic event of apoptosis), whereas nearby nontransfected cells retained their native morphology (Figure 10c, d).[17] Thus, a cascade of events taking place in

DOI: 10.1021/acsami.5b05280
ACS Appl. Mater. Interfaces 2015, 7, 18717−18731

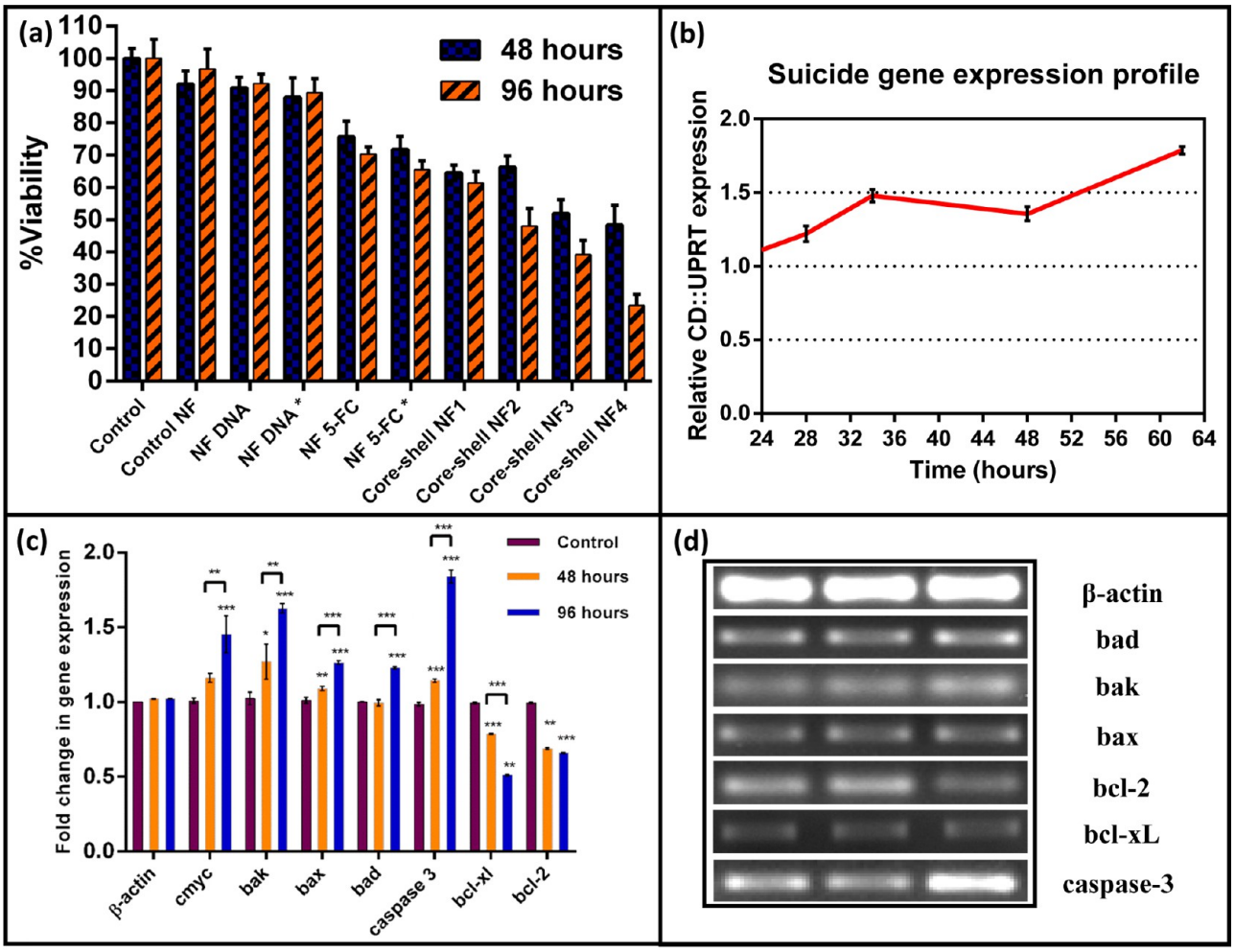

Figure 12. (a) A549 cell viability after 48 and 96 h of seeding over core−shell nanofibers loaded with suicide gene and prodrug, (b) level of CD-UPRT gene expression by transfected A549 cells at different time points, (c, d) relative gene expression profile of apoptotic genes at 48 and 96 h.

CD::UPRT suicide gene therapy commends that higher transfection efficiency is not a prerequisite for attaining effective GDEPT against cancer cells.

3.8. RBP Polyplex Cellular Uptake. The representative images depicting RBP polyplex release from core−shell nanofibers followed by its attachment onto the cell membrane during the initial stages of incubation could be captured effectively by FE-SEM (Figure 10a, b). As evident from FE-SEM images, RBP polyplexes were intact and uniform in morphology even after release from core−shell nanofibers.

3.9. Monitoring Suicide Gene Therapy by Flow Cytometer. A gradual shift in cell population was observed as the suicide gene therapy progressed, which was quantified by a flow cytometer at different time points (Figure 11). The total cell population was classified by flow cytometer as % live or dead cells and % transfected cell or nontransfected A549 cells. The transfected cells expressing GFP were monitored by its green fluorescence in Ch02, whereas nontransfected cells appeared only in Ch01 (brightfield image) alone. The dead cell nucleus stained with PI was distinctly visible in Ch04 when excited by a 488 nm laser. Both GFP and PI were excited by a 488 laser with the power optimized to a value sufficient to detect green fluorescence of transfected cells and at the same time not high enough to saturate PI stained cells. After 24 h, around 3.43% of GFP/CD::UPRT transfected cells were alive and 1.84% of GFP/CD::UPRT were dead. As compared to the control nanofibers, cell viability was reduced by 13.3% by the end of 24 h in the case of RBP and 5-FC loaded core−shell nanofibers. The cell viability difference arises partly because of GFP/CD::UPRT suicide gene and the rest because of 5-FC and bPEI toxicity. Subsequently at 36 h, the fraction of live transfected cells increased to 6.81% along with a corresponding increase in dead transfected cells (i.e., from 1.84% at 24 h to 3.06% at the end of 36 h). The cell viability was further reduced to 63.41% by the end of 36 h which also included 6.81% of cells expressing GFP/CD::UPRT suicide gene. As an outcome of A549 cells expressing suicide gene (i.e., 6.81% at 36 h), a drastic decline in cell viability was observed at 72 h, that is, 46.11% (39.9% nontransfected live cells and 6.21% transfected live cells). With an increasing time span of incubation, cell population migrates from III quadrant (nontransfected) to IV (dead cells) and II quadrant (transfected cells). Moreover, a few transfected cells which have completely lost the membrane integrity lose GFP proteins too and, thus, could also migrate from quadrant IV to II straightaway instead of staying in quadrant I. Although the percentage of transfected cells was almost the same at 36 and 72 h, there was a significant increase in percentage of dead transfected cells (i.e., from 3.06% to 11.6%) clearly indicating that sustained release of RBP polyplexes and transfection of new A549 cells replenishes the

DOI: 10.1021/acsami.5b05280
ACS Appl. Mater. Interfaces 2015, 7, 18717−18731

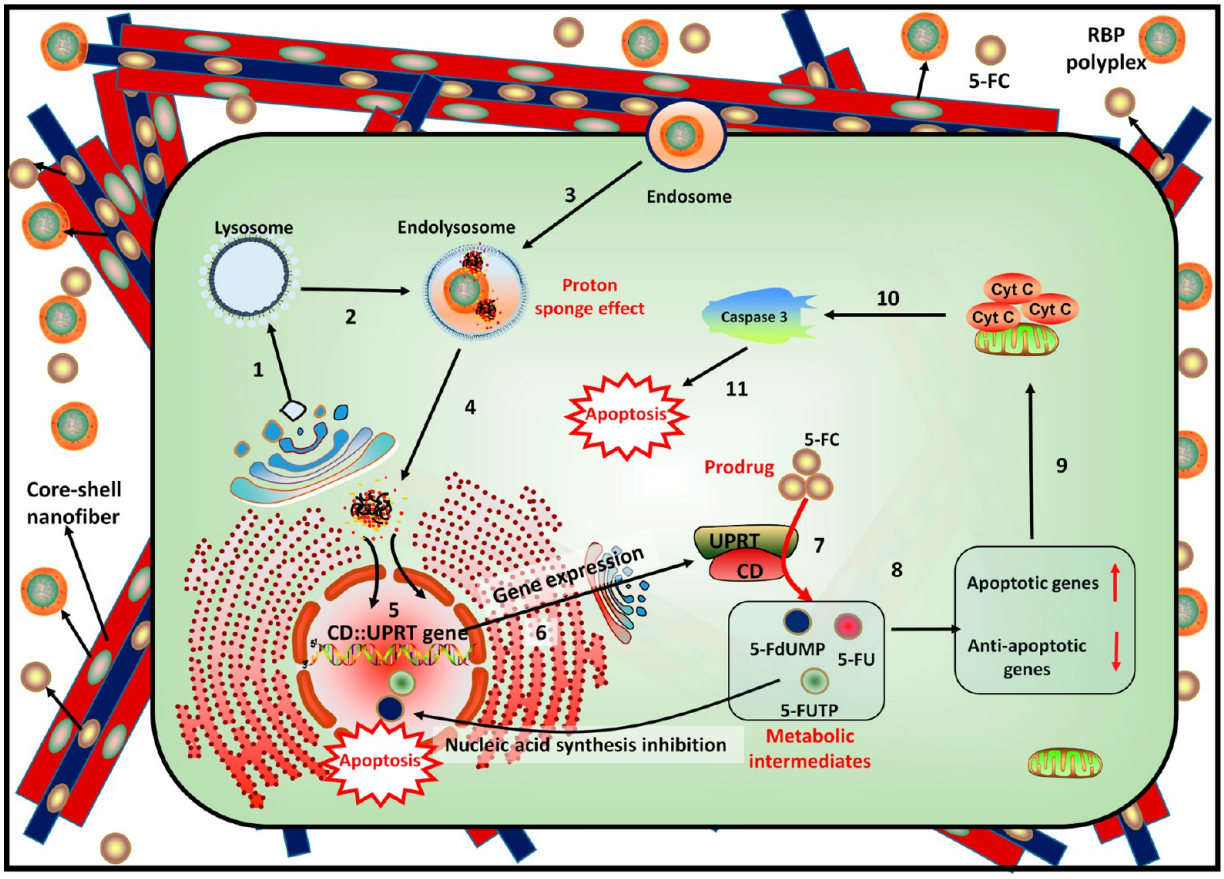

Figure 13. Schematic outline of suicide gene therapy mediated by core−shell nanofibers loaded with RBP polyplexes and 5-FC. Steps 1−7 are common entry pathways for RBP polyplexes followed by steps 8−11 which indicates p53 mediated apoptotic pathway usually followed by most of the anticancer drugs.

dead transfected cells up to 72 h. The core−shell control nanofibers loaded with RBP alone accounted for 16.5% GFP/CD::UPRT suicide gene transfection in A549 cells by the end of 72 h. At the outset, it is these 16.5% of transfected cells that account for almost 34% decline in cell viability. The difference in percent of transfected cells and dead cells (i.e., 34% − 16.5% = 17.5%) arises solely because of the bystander effects of CD::UPRT.

3.10. Cell Viability Assay. Only a negligible difference in cell viability was observed between core−shell nanofibers loaded with different extents of RBP (0.11 and 0.22 wt %) or 5-FC (0.25 and 0.5 wt %), that is, 1.79% and 3.63%, respectively, by the end of 48 h (Figure 12a). Absence of such cell viability difference at 48 h arises because of delayed transfection of CD::UPRT suicide gene which could effectively mediate antiproliferative effects at later stages only (i.e., after 48 h). Thus, at later stages, that is, at 96 h, the cell viability difference widened further as all transfected A549 cells underwent apoptosis in the presence of prodrug 5-FC and also augmented the bystander effects. As expected, with an increase in concentration of either RBP polyplexes or 5-FC, the cell viability decreased independently. Moreover, different polyplex concentrations could attain higher cell viability differences (i.e., 15.78% between core−shell NF3 and NF4) as compared to those with different 5-FC concentrations (13.39% between core−shell NF1 and NF2). This observation indicates that, although transfection % and 5-FC concentration augment each other in mediating apoptosis, the percent of transfected cells has better influence on cell viability as compared to concentration of 5-FC. The core−shell NF4 loaded with higher limits of RBP polyplexes and 5-FC (core−shell NF4) could manifest the lowest cell viability at 96 h.

3.11. Gene Expression Studies. Semiquantitative RT-PCR analysis of RNA isolated from treated A549 cells at different time points confirmed genomic integration and expression of CD::UPRT suicide gene. With passage of time, expression of suicide gene gradually increases indicating greater fraction of transfected cells (Figure 12b). Apart from suicide gene expression, relative expression of apoptotic genes was also quantified for treated A549 cells at 48 and 96 h. As observed in cell viability assay, no significant difference in expression of pro-apoptotic or antiapoptotic gene expression was observed until 48 h, whereas at 96 h significant up-regulation of apoptotic genes and consequent down-regulation of antiapoptotic genes was observed (Figure 12c, d). Apoptotic genes c-myc, bak, and caspase 3 expressions were up-regulated very prominently as compared to the rest, which is clearly indicative of apoptosis. Pre-existing literature also supports CD::UPRT/5-FC mediated up-regulation of pro-apoptotic genes as observed in this work.[18] The translated products of bax, bad, and bak genes generate oligomeric pores in the outer membrane of mitochondria as an outcome of which cytochrome *c* present within mitochondria is released. The cytochrome *c* present in the cytosol further activates the caspase family of genes leading to nuclear genome fragmentation which is the characteristic feature of cells undergoing apoptosis.[19] Activation of apoptotic gene cascade instigates interplay of multiple pathways which ultimately culminates in apoptosis.[20]

DOI: 10.1021/acsami.5b05280
ACS Appl. Mater. Interfaces 2015, 7, 18717−18731

4. CONCLUSION

The core−shell nanofiberous scaffold fabricated in this work has been validated to attain independent delivery of both suicide gene and prodrug in a controlled and sustained manner over a prolonged time span. In the initial stages, RhoB tagged RBP polyplexes present in the nanofiber shell were released, leading to transfection and expression of suicide gene CD::UPRT in A549 cells (Figure 13). Henceforth, gradual increase in A549 cells expressing GFP/CD::UPRT gene was monitored with the passage of time. The prodrug (5-FC) loaded in the nanofiber core was subsequently released which was later transformed into toxic metabolites (5-FU, 5-FUMP, 5-FdUMP, 5-FUTP) when acted upon by CD::UPRT enzyme expressed by transfected A549 cells. The time lag attained between delivery of RBP polyplexes and prodrug 5-FC also favors improved therapeutic efficacy. Apart from inducing apoptosis in transfected A549 cells, CD::UPRT suicide gene could also effectively mediate bystander effects to cells in the vicinity which further augments therapeutic efficacy of suicide gene therapy. Moreover, time-dependent antiproliferative effects of suicide gene therapy were ascertained on qualitative and quantitative basis by various staining procedures and assays. Such versatile core−shell nanofiber scaffold for subsequent delivery of suicide gene and prodrug has been attained for the first time, and thus, this work opens up new application for an ever expanding field of nanofiberous scaffolds.

■ ASSOCIATED CONTENT

Supporting Information

The Supporting Information is available free of charge on the ACS Publications website at DOI: 10.1021/acsami.5b05280.

Gene-specific primers used for apoptotic gene expression studies, DNase I protection assay, and schematic representation of gluteraldehyde mediated cross-linking reaction (PDF)

■ AUTHOR INFORMATION

Corresponding Author

*Tel: +91-1332-285650. Fax: +91-1332-273560. E-mail: pgopifnt@iitr.ernet.in; genegopi@gmail.com.

Notes

The authors declare no competing financial interest.

■ ACKNOWLEDGMENTS

This work was supported by the Science and Engineering Research Board (No. SR/FT/LS-57/2012), Department of Biotechnology (No. BT/PR6804/GBD/27/486/2012), and Ministry of Human Resource Development (Faculty initiation grant, IIT Roorkee), Government of India. S.U.K. is thankful to the Ministry of Human Resource Development, Government of India, for the fellowship. Sincere thanks to Department of Chemistry and Institute Instrumentation Centre, IIT Roorkee, for the various analytical facilities provided.

■ REFERENCES

(1) Lee, S.; Jin, G.; Jang, J. H. Electrospun Nanofibers as Versatile Interfaces for Efficient Gene Delivery. *J. Biol. Eng.* **2014**, *8*, 30−34.

(2) Vasita, R.; Katti, D. S. Nanofibers and their Applications in Tissue Engineering. *Int. J. Nanomedicine* **2006**, *1* (1), 15−30.

(3) Alekseenko, I. V.; Snezhkov, E. V.; Chernov, I. P.; Pleshkan, V. V.; Potapov, V. K.; Sass, A. V.; Monastyrskaya, G. S.; Kopantzev, E. P.; Vinogradova, T. V.; Khramtsov, Y. V.; Ulasov, A. V.; Rosenkranz, A. A.; Sobolev, A. S.; Bezborodova, O. A.; Plyutinskaya, A. D.; Nemtsova, E. R.; Yakubovskaya, R. I.; Sverdlov, E. D. Therapeutic Properties of a Vector Carrying the HSV Thymidine Kinase and GM-CSF Genes and Delivered as a Complex with a Cationic Copolymer. *J. Transl. Med.* **2015**, *13* (1), 78.

(4) Duarte, S.; Carle, G.; Faneca, H.; de Lima, M. C.; Pierrefite-Carle, V. Suicide Gene Therapy in Cancer: Where Do We Stand Now? *Cancer Lett.* **2012**, *324* (2), 160−170.

(5) Gopinath, P.; Ghosh, S. S. Implication of Functional Activity for Determining Therapeutic Efficacy of Suicide Genes In Vitro. *Biotechnol. Lett.* **2008**, *30* (11), 1913−1921.

(6) Kucerova, L.; Altanerova, V.; Matuskova, M.; Tyciakova, S.; Altaner, C. Adipose Tissue-Derived Human Mesenchymal Stem Cells Mediated Prodrug Cancer Gene Therapy. *Cancer Res.* **2007**, *67* (13), 6304−13.

(7) Altaner, C.; Altanerova, V.; Cihova, M.; Ondicova, K.; Rychly, B.; Baciak, L.; Mravec, B. Complete Regression of Glioblastoma by Mesenchymal Stem Cells Mediated Prodrug Gene Therapy Simulating Clinical Therapeutic Scenario. *Int. J. Cancer* **2014**, *134* (6), 1458−1465.

(8) Hsu, C. Y.; Uludag, H. A Simple and Rapid Nonviral Approach to Efficiently Transfect Primary Tissue-derived Cells Using Polyethylenimine. *Nat. Protoc.* **2012**, *7* (5), 935−45.

(9) Benjaminsen, V. R.; Mattebjerg, M. A.; Henriksen, J. R.; Moghimi, S. M.; Andresen, T. L. The Possible "Proton Sponge" Effect of Polyethylenimine (PEI) Does Not Include Change in Lysosomal pH. *Mol. Ther.* **2013**, *21* (1), 149−157.

(10) Kumar, S. U.; Gopinath, P. Controlled Delivery of bPEI-Niclosamide Complexes by PEO Nanofibers and Evaluation of its Anti-Neoplastic Potentials. *Colloids Surf., B* **2015**, *131*, 170−181.

(11) Lambert, J. B. *Introduction to Organic Spectroscopy*; Macmillan: New York, 1987; ISBN 0023673001.

(12) Shen, S. L.; Chen, X. P.; Zhang, X. F.; Miao, J. Y.; Zhao, B. X. A Rhodamine Based Lysosomal pH Probe. *J. Mater. Chem. B* **2015**, *3*, 919−924.

(13) Denny, W. A. Prodrugs for Gene-Directed Enzyme-Prodrug Therapy (Suicide Gene Therapy). *J. Biomed Biotechnol.* **2003**, *1*, 48−70.

(14) Kumar, S. U.; Matai, I.; Dubey, P.; Bhushan, B.; Sachdev, A.; Gopinath, P. Differentially Cross-Linkable Core−Shell Nanofibers for Tunable Delivery of Anticancer Drugs: Synthesis, Characterization and their Anticancer Efficacy. *RSC Adv.* **2014**, *4*, 38263.

(15) Blau, A. Cell Adhesion Promotion Strategies for Signal Transduction Enhancement in Microelectrode Array In Vitro Electrophysiology: An Introductory Overview and Critical Discussion. *Curr. Opin. Colloid Interface Sci.* **2013**, *18* (5), 481−492.

(16) Lee, C. H.; Ni, Y. H.; Chen, C. C.; Chou, C. K.; Chang, F. H. Synergistic Effect of Polyethylenimine and Cationic Liposomes in Nucleic Acid Delivery to Human Cancer Cells. *Biochim. Biophys. Acta, Biomembr.* **2003**, *1611* (1−2), 55−62.

(17) Coleman, M. L.; Sahai, E. A.; Yeo, M.; Bosch, M.; Dewar, A.; Olson, M. F. Membrane Blebbing during Apoptosis Results from Caspase-Mediated Activation of ROCK I. *Nat. Cell Biol.* **2001**, *3* (4), 339−345.

(18) Gopinath, P.; Ghosh, S. S. Apoptotic Induction with Bifunctional E. Coli Cytosine Deaminase-Uracil Phosphoribosyltransferase Mediated Suicide Gene Therapy is Synergized by Curcumin Treatment In Vitro. *Mol. Biotechnol.* **2008**, *39* (1), 39−48.

(19) Aluvila, S.; Mandal, T.; Hustedt, E.; Fajer, P.; Choe, J. Y.; Oh, K. J. Organization of the Mitochondrial Apoptotic BAK Pore: Oligomerization of the BAK Homodimers. *J. Biol. Chem.* **2014**, *289* (5), 2537−2551.

(20) Gopinath, P.; Ghosh, S. S. Understanding Apoptotic Signaling Pathways in Cytosine Deaminase-Uracil Phosphoribosyl Transferase-Mediated Suicide Gene Therapy In Vitro. *Mol. Cell. Biochem.* **2009**, *324* (1−2), 21−29.

DOI: 10.1021/acsami.5b05280
ACS Appl. Mater. Interfaces 2015, 7, 18717−18731